Unsteady Boundary Layers on a Flat Plate Disturbed by Periodic Wakes: Part I—Measurement of Wake-Affected Heat Transfer and Wake-Induced Transition Model

K. Funazaki
Department of Mechanical Engineering,
Iwate University,
Morioka, Iwate,
Japan

Measurements of wake-affected heat transfer distributions on a flat plate are made by use of a wake generator that consists of a rotating disk and several types of circular cylinder. The main purpose of this study is to construct a wake-induced transition model in terms of an intermittency factor, considering the evolution of the wake-induced turbulent region, a so-called turbulent patch in a distance–time diagram. A comparison between the proposed transition model and the measured heat transfer data reveals that the transition model yields good agreement with the measured data of all test conditions in this study.

Introduction

Transition phenomena in gas turbine engines have been one of the most important issues facing aerodynamists as well as cooling designers of turbine blades. Recently, wake-induced transition of boundary layers over blade surfaces has received much attention from a large number of researchers. Considerable amounts of observation about transition phenomena have been made, for example by Pfeil and Herbst (1979), Pfeil et al. (1983), LaGraff et al. (1989), Addison and Hodson (1990a, b), and Dullenkopf et al. (1991), and accordingly several models of the wake-induced transition are proposed in a somewhat phenomenological fashion by Addison and Hodson (1992), Dong and Cumpsty (1990) or in semi-analytical ways by Addison and Hodson (1990a, b), Mayle and Dullenkopf (1990, 1991). In a practical sense, the Mayle–Dullenkopf model seems to be useful for predicting wake-affected heat transfer along a blade surface, which is described in terms of the intermittency factor as follows:

$$\gamma_w(x) = 1 - \exp\left[-C\left(\frac{x - x_w}{U_\infty T}\right)\right], \quad C = 1.9 \qquad (1)$$

where x_{tw} is a wake-induced transition point, U_∞ is a free-stream velocity and T is a wake-passing period. This Mayle–Dullenkopf model, which was developed on the basis of a statistical approach by Emmons (1951) in conjunction with some experimental data, reportedly yielded good agreements with the experimental data employed in their studies.

On the other hand, Funazaki et al. (1993) conducted an experimental simulation for wake–blade interaction, using a bar-type wake generator and a flat plate, in order to investigate wake-affected heat transfer distributions over the plate surface with no pressure gradient, whose results were then compared with the Mayle–Dullenkopf model. Consequently, it was found that the wake-affected heat transfer distributions obtained in several cases of the wake-passing frequency could not be adequately reproduced by Eq. (1) with no manipulation of the constant C in Eq. (1), x_{tw} being regarded as a constant for a fixed Reynolds number. In addition, in the highest wake-passing frequency, any attempts using the Mayle–Dullenkopf model failed to produce a reasonable agreement with the experimental data. A similar finding is recently reported by Han et al. (1993). Using the results obtained, Funazaki et al. proposed another transition model. It was based on the evolution of wake-induced turbulent spots (or turbulent patch) in the distance–time diagram as shown in Fig. 1, which was similar to that of Pfeil et al. (1983). Their transition model is expressed as follows:

$$\gamma_w(x) = \left(\frac{1}{U_E} - \frac{1}{U_F}\right)\frac{x - x_{tw}}{T} = \left(\frac{1}{\beta_E} - \frac{1}{\beta_F}\right)\frac{x - x_{tw}}{L} S$$

$$S = \frac{L}{U_\infty T},$$

where $U_E \equiv \beta_E U_\infty$ and $U_F \equiv \beta_F U_\infty$ are propagation speeds of the preceding and following portions of the turbulent patch. Note that the values of coefficients β_E and β_F are assumed to be 0.55 and 1.0, respectively. It was somewhat surprising to see that this simple transition model successfully predicted the wake-affected heat transfer distributions for all of the unsteady flow conditions employed in that study, where the wake-induced transition point was experimentally determined.

Although the proposed model in Eq. (2) is verified to yield a reasonable prediction of wake-affected heat transfer on a flat plate surface with no pressure gradient, there still remain several points to be considered for a more accurate and reliable transition model. For example, the effects of incident wake characteristics, e.g., turbulence intensity involved within the wake or wake duration, on the transition are not fully discussed. Furthermore, there is no clear criterion of a wake-induced transition point to date.

Contributed by the International Gas Turbine Institute and presented at the 39th International Gas Turbine and Aeroengine Congress and Exposition, The Hague, The Netherlands, June 13–16, 1994. Manuscript received by the International Gas Turbine Institute February 24, 1994. Paper No. 94-GT-429. Associate Technical Editor: E. M. Greitzer.

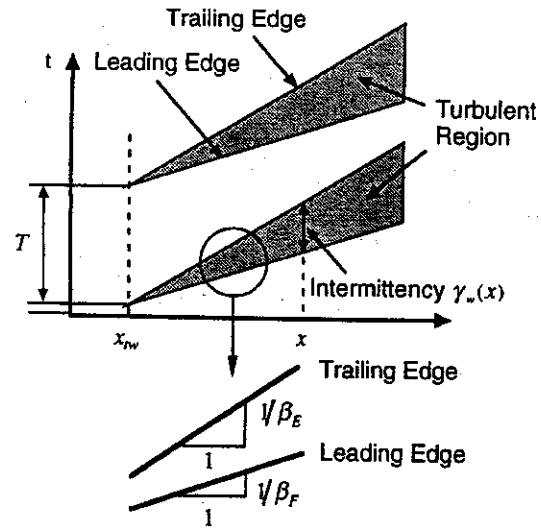

Fig. 1 Schematic of wake-induced transition model in a distance-time diagram (Funazaki et al., 1993)

Accordingly, the emphasis of this experimental study as Part I is placed on the investigation of the wake characteristics effects, from which results are utilized to develop a more accurate wake-induced transition model. In Part II, the onset of the transition will be argued on the basis of the hot-wire measurements of the unsteady transitional boundary layers in conjunction with the heat transfer data obtained in Part I.

Experimental Investigation

Test Apparatus. A brief explanation on the test apparatus and the measurement system is made, because it is largely the same as the previous study of Funazaki et al. (1993). Figure 2 shows the test apparatus used in this study. Air from the nozzle with a speed of 30 m/s and a turbulence intensity less than 1.0 percent is fed to the test section through the wake generator, as shown in the lower portion of Fig. 2. This wake generator consists of a rotating disk with diameter of 400 mm and several

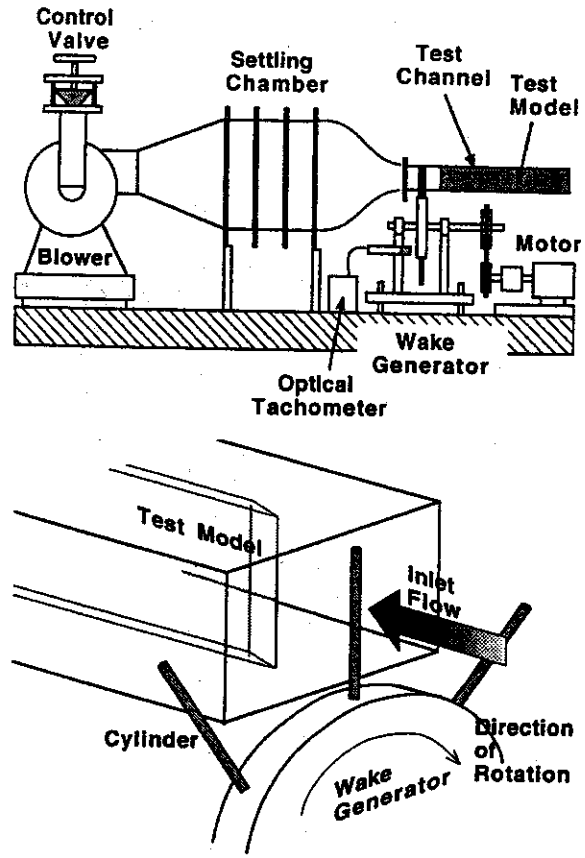

Fig. 2 Test apparatus (upper), wake generator (lower)

circular cylinders attached on the disk rim. Three types of cylinders with different diameters, i.e., 2 mm, 5 mm, and 10 mm, are used to observe how such differences in wake characteristics can affect the wake-induced transition. The test section is a rectangular acrylic resin duct with 120 mm × 240 mm cross section and has slots through which the cylinders can pass. The rotational speed of the disk is changed with a transmission gear

Nomenclature

d = diameter of cylinder
f = wake passing frequency
h = heat transfer coefficient
L = length of the flat plate
l_D = distance between the wake generating cylinder and the leading edge of the flat plate
max[ ], min[ ] = functions that select maximum and minimum values from the values in the brackets
n = revolution number
n_c = number of cylinders
$\dot{q}_w$, $\dot{q}_{loss}$, $\dot{q}_{supply}$ = surface heat flux, heat loss, supplied heat flux
Re = Reynolds number = $U_\infty L/\nu$
Re_x = Reynolds number based on the length measured from the leading edge of the plate
Re_θ = momentum thickness Reynolds number
S = Strouhal number
S_w = wake passing Strouhal number = $L/(U_\infty T)$
St(x) = local Stanton number
$\mathrm{St}_{NW}(x)$ = local Stanton number obtained in the no-wake case
$\mathrm{St}_T(x)$ = local Stanton number obtained in the fully turbulent case
T = wake passing period
t = time
Tu = ensemble-averaged turbulence intensity
$T_w(x)$, T_∞ = local surface temperature, free-stream temperature
U_E, U_F = trailing edge and leading edge propagation velocities of turbulent spot
U_∞ = free-stream velocity
$v(t_j)$ = instantaneous velocity
$\tilde{v}(t_j)$, $v'^2(t_j)$ = ensemble-averaged velocity, ensemble-averaged variation of velocity
x = surface length from the leading edge
x_{tw} = start point of forced transition
y = distance from the plate surface
$\gamma_w(x)$ = wake-induced local intermittency factor of the boundary layer
τ_w = wake duration time

Subscripts

NW = no wake
T = turbulent

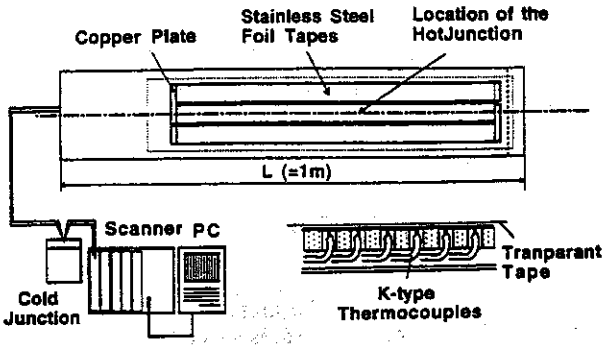

Fig. 3 Test model for heat transfer measurement, showing the installation of the thermocouples

box connected to the induction motor and is sensed by an optical tachometer. Flow rate through the test section can be controlled by the valve of the blower intake and is monitored by a Pitot tube installed at the duct.

A sharp-edged flat plate of 1000 mm length and 10 mm thickness is used for the measurement of the heat transfer rate; it is placed within the duct aligned almost along its centerline. The distance between the plate and the wake generator, l_D, is usually fixed to be 0.12 m, but it can be changed in order to vary wake characteristics, e.g., wake depth, on the flat plate. Sixty equally spaced holes of 5 mm diameter are drilled through the plate along the center line. As shown in Fig. 3, each of the holes is plugged with urethane foam and a hot junction of K-type (chromel-alumel) thermocouple is then flush-mounted on the surface to be measured, penetrating back through the foam. The wires of the thermocouples are buried inside a slot on the back of the plate. Both sides of the plate are covered with stainless steel foil adhesive tapes of 30 μm thickness, which are soldered onto copper plates and heated by electricity. For the purpose of preventing the buckling of the foils during heating, transparent tapes (3M Book Tape 845, 90 μm thickness) is pasted on the stainless foils. Temperature drop through this tape is about 0.025°C.

Smooth inflow to the flat plate is achieved by adjusting the open area of the duct exit, which is confirmed by the oil flow pattern on the plate. This is also the case in the unsteady flow conditions since even in the wake the inflow has a slight negative incidence to the measured surface of the plate at most and causes no flow separation around the leading edge.

Measuring System

Wake Characteristics. Figure 4(a) shows the wake measuring system in this study. An I-type hot-wire probe (Kanomax, Model 0251R) is used not only to detect the wake profile in front of the flat plate, but also to investigate the streamwise variation of wake characteristics above the plate, as will be shown in Fig. 5. Signals from the hot-wire probe are processed by a constant-temperature anemometer (Kanomax, System 7201) and the linearized signals are then A/D converted by the computer-controlled digitizer (Autonix, APC-204), with a sampling frequency of 50 kHz and memory size of the logged data per process 2048 words. Each of the data-acquisition processes is triggered by a signal from the optical tachometer, which yields test data synchronized with the disk revolution.

For one test condition, 256 lines of time-serial digitized data for velocity, $v_i(t_j)$ (j = 1, . . . , 2048), are logged. They are transferred back to the computer, and then stored in the auxiliary memory unit for subsequent off-line calculation, as described in the following.

Ensemble-averaged velocity $\tilde{v}_i(t_j)$ and its variance $v'^2(t_j)$ are calculated as

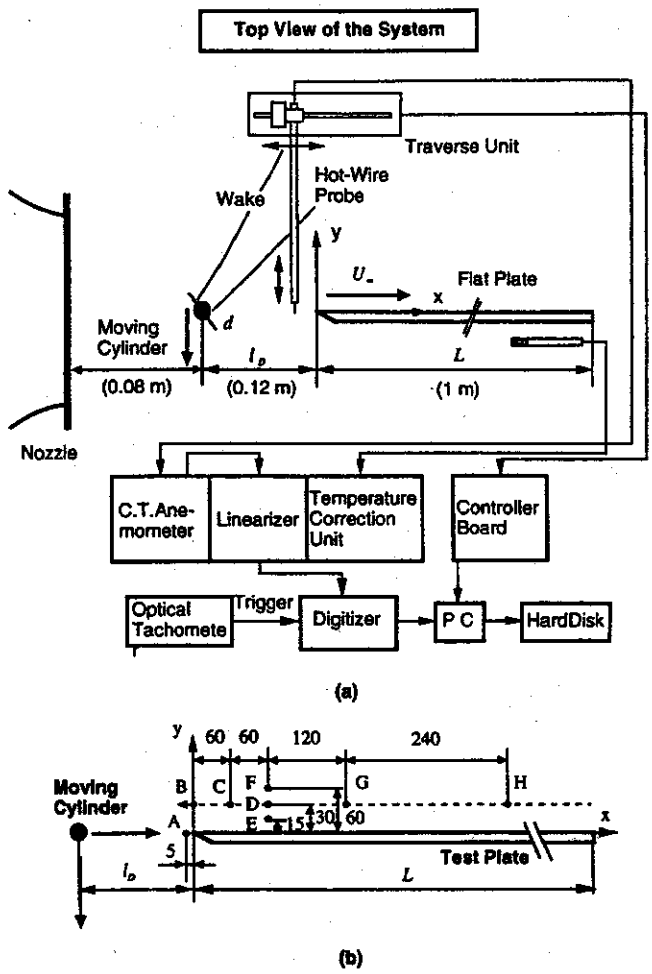

Fig. 4 (a) Measuring system (upper); (b) locations for the wake profile measurement (lower)

$$\tilde{v}(t_j) = \frac{1}{k}\sum_{i=1}^{k} v_i(t_j), \quad k = 256 \tag{3}$$

$$v'^2(t_j) = \frac{1}{k-1}\sum_{i=1}^{k} [v_i(t_j) - \tilde{v}(t_j)]^2. \tag{4}$$

Local turbulence intensity is then defined as

$$Tu(t_j) = \frac{\sqrt{v'^2(t_j)}}{U_\infty}. \tag{5}$$

Heat Transfer. After confirming thermal equilibrium conditions by monitoring the surface temperature distribution, the signals from all the thermocouples embedded in the flat plate

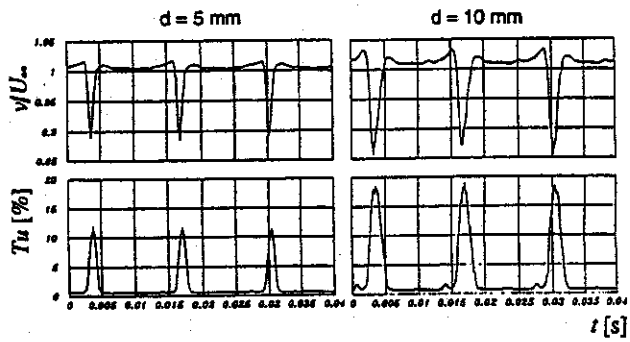

Fig. 5 Ensemble-averaged wake profiles obtained at point A in Fig. 4 for d = 5 mm and d = 10 mm

are scanned 10 times during about 30 seconds. They are then averaged for each measuring point to obtain time-averaged heat transfer characteristics, i.e., Stanton number distribution St or heat transfer coefficient distribution h, which are determined as follows:

$$\mathrm{St}(x) = \frac{\dot{q}_w}{c_p U_\infty (T_w(x) - T_\infty)} = \frac{\dot{q}_{\text{supply}} - \dot{q}_{\text{loss}}}{c_p U_\infty (T_w(x) - T_\infty)} \quad (6)$$

$$h(x) = \frac{\dot{q}_w}{(T_w(x) - T_\infty)} = \frac{\dot{q}_{\text{supply}} - \dot{q}_{\text{loss}}}{(T_w(x) - T_\infty)}, \quad (7)$$

where $T_w(x)$ is the time-averaged surface temperature, T_∞ is the free-stream temperature measured at the aft portion of the test section, and $\dot{q}_w$ is the surface heat flux. Preliminary experiments determined the correlation for the heat flux $\dot{q}_{\text{loss}}$ that did not contribute to the convective heat transfer. Attention was paid to maintaining the same level of the average of the temperature difference $T_w(x) - T_\infty$ almost constant ($\approx$ 10°C) in every test run as well as to avoiding overheating of the foils, because the air temperature sometime rose to more than 30°C. Average uncertainty in the Stanton number is estimated by the method of Kline and McClintock (1953) and is about $\pm$ 7 percent.

Results

Wake Profiles. Figure 4(*b*) shows the locations of wake measurement points around the test plate. Wake profiles obtained ahead of the leading edge of the plate (point A in Fig. 4(*b*)) are presented in Fig. 5 for the two wake-generating cylinders, which are expressed in terms of the ensemble-averaged velocity distribution as well as the ensemble-averaged turbulence intensity distribution with respect to time. Maximum values of turbulence intensity measured within the wakes, $Tu_{\max}$, for the cylinders with diameters of 2 mm, 5 mm, and 10 mm are about 6, 12, and 18 percent, respectively. These values are found to be almost unchanged even at a doubled rotational speed of the disk in the wake generator. It is also discovered that the turbulence intensity distributions, not in a rigorous sense, can be approximated by a Gaussian distribution, namely

$$Tu(t) = \max\left[Tu_b, Tu_{\max} \exp\left(-\ln 2\left(\frac{t}{\tau_{1/2}}\right)^2\right)\right], \quad (8)$$

where Tu_b is a background turbulence intensity, i.e., free-stream turbulence intensity; $\tau_{1/2}$ is a semi-depth width for a turbulence intensity profile. From a comparison between the velocity profiles and the turbulence intensity profiles, it is found that a semi-depth width for the turbulence intensity profile is about 1.5 times as large as that of the corresponding velocity profile, that is,

$$\tau_{1/2,Tu} \cong 1.5\tau_{1/2,\text{velocity}}. \quad (9)$$

Measurements at several points in Fig. 5 demonstrate some of the wake profile variations in the streamwise and crossflow direction. Figures 6(*a*) and (*b*), in the cases of 5-mm and 10-mm-dia cylinders, show streamwise variations of wake profiles measured along the plane with 30 mm distance from the test plate surface. Despite the streamwise wake decay, wakes measured at the farthest point downstream from the leading edge still retain considerable amount of the turbulence intensities. In the velocity profiles of the wakes, shown in the upper portion of each of the graphs, there always appears a slight acceleration before the velocity deficit. Such acceleration tends to be pronounced in the case of larger cylinder diameter, as well as in the case of closer measurement point to the plate surface as shown in Figs. 7(*a*) and 7(*b*). Meyer (1957) explained these phenomena as a negative jet effect. One of the interesting findings in Fig. 7 is that the turbulence intensity profiles within the wakes do no exhibit any drastic changes even when the measurement point moves close to the wall, in contrast to the corresponding velocity profiles, which suffer from deformation so severely that one may not identify the extent of the wake correctly. Hence, the present author holds that wake characteristics, e.g., wake duration, must be defined in terms of turbulence intensity, not velocity.

Wake-Affected Heat Transfer

Effect of Wake-Passing Frequency. It is understood from the previous studies by Mayle and Dullenkopf (1990) as well as by Funazaki et al. (1993) that wake-affected heat transfer becomes more enhanced in the higher wake-passing frequencies. This is also the case in the present study as shown in Figs. 8(*a*) for the 5-mm-dia case and 8(*b*) for the 10-mm-dia case. In these figures the data referred to as "Turbulent" were obtained with one of the cylinders on the disk rim being fixed just in front of the plate leading edge so that the wake from that cylinder covers the plate surface all the time, while the data referred to as "No Wake" mean the heat transfer distribution under no-wake flow condition. It should be noted that an inlet Reynolds number, Re ($= U_\infty L/\nu$) adopted in this study is unchanged and is 2×10^6 for all cases. Also shown in these figures are the results obtained from the correlations for constant surface heat flux case given by Kays and Crawford (1980), which are for a laminar boundary layer,

$$\mathrm{St} = 0.453\mathrm{Pr}^{-2/3}\mathrm{Re}_x^{-1/2}, \quad (10)$$

and for a turbulent boundary layer,

$$\mathrm{St} = 0.0287\mathrm{Pr}^{-0.4}\mathrm{Re}_x^{-0.2}. \quad (11)$$

Note that the unheated starting length ($\cong$ 0.04 m) is taken into account for both cases. The obtained Stanton numbers for the "No Wake" and the "Turbulent" mostly follow Eqs. (10) and (11), although slight differences appear.

By changing the disk rotational speed from 900 rpm to 1500 rpm, which corresponds to Strouhal numbers ranging from 1.5 to 2.5, the measured Stanton number distributions along the surface accordingly increase from the base line data, i.e., "steady flow," toward the turbulent flow case. This means that the boundary layer under the influence of the periodic wakes is in a transitional state and such wakes surely promote earlier transition of the boundary layer. At the highest wake-passing frequency, as shown in Fig. 9, the boundary layer completes its transition process so quickly that a larger portion of the test plate is covered with the turbulent boundary layer. Figure 10 demonstrates dominant effects of the wake-passing frequency on the wake-affected heat transfer. In such a case, remarkable agreement is obtained between the two heat transfer distributions under the same wake-passing frequency, even though combinations of the disk rotation speed and the number of cylinders on the disk rim are quite different.

Effect of Cylinder Diameter. Quantitative differences in heat transfer enhancement by wakes became very obvious among the experimental data obtained for the three different cylinders. Such a difference is more visible in Fig. 11. It is not difficult to predict this difference when recalling the above-mentioned large differences in the wake characteristics, but the present author would like to draw the readers' attention to the point that the original Mayle–Dullenkopf model of Eq. (1) as well as the previously proposed model of Eq. (2) takes no account of any information about the wake structure in an explicit manner. Therefore, they cannot explain the difference in heat transfer without manipulation of the transition point, x_{tw}. In the next section, it will be shown that Eq. (2) can be modified in a very simple fashion to include effects originating from the wake structure.

Effect of the Distance Between the Test Plate and the Moving Cylinders. Figure 12 shows a sample of wake-affected heat transfer distributions obtained by changing the distance between

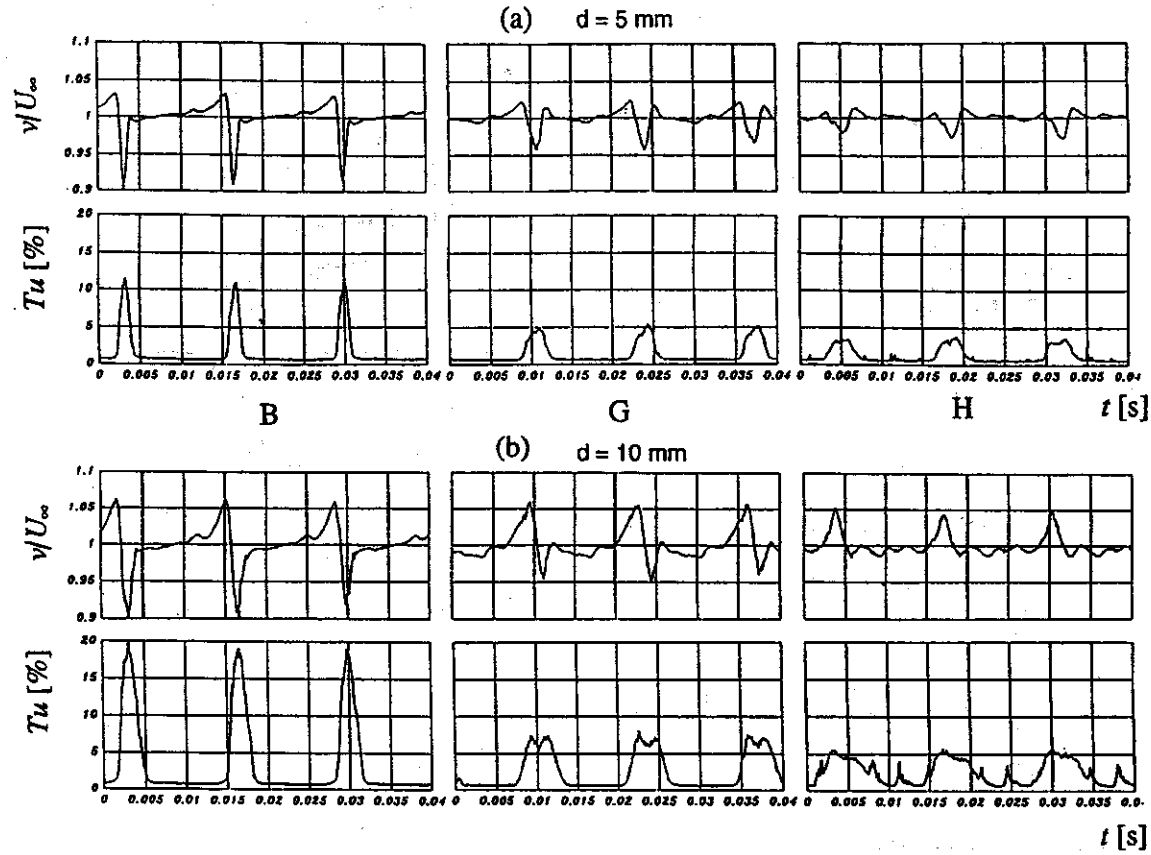

Fig. 6 Streamwise variations of the ensemble-averaged wake profiles: (*a*) d = 5 mm, (*b*) d = 10 mm

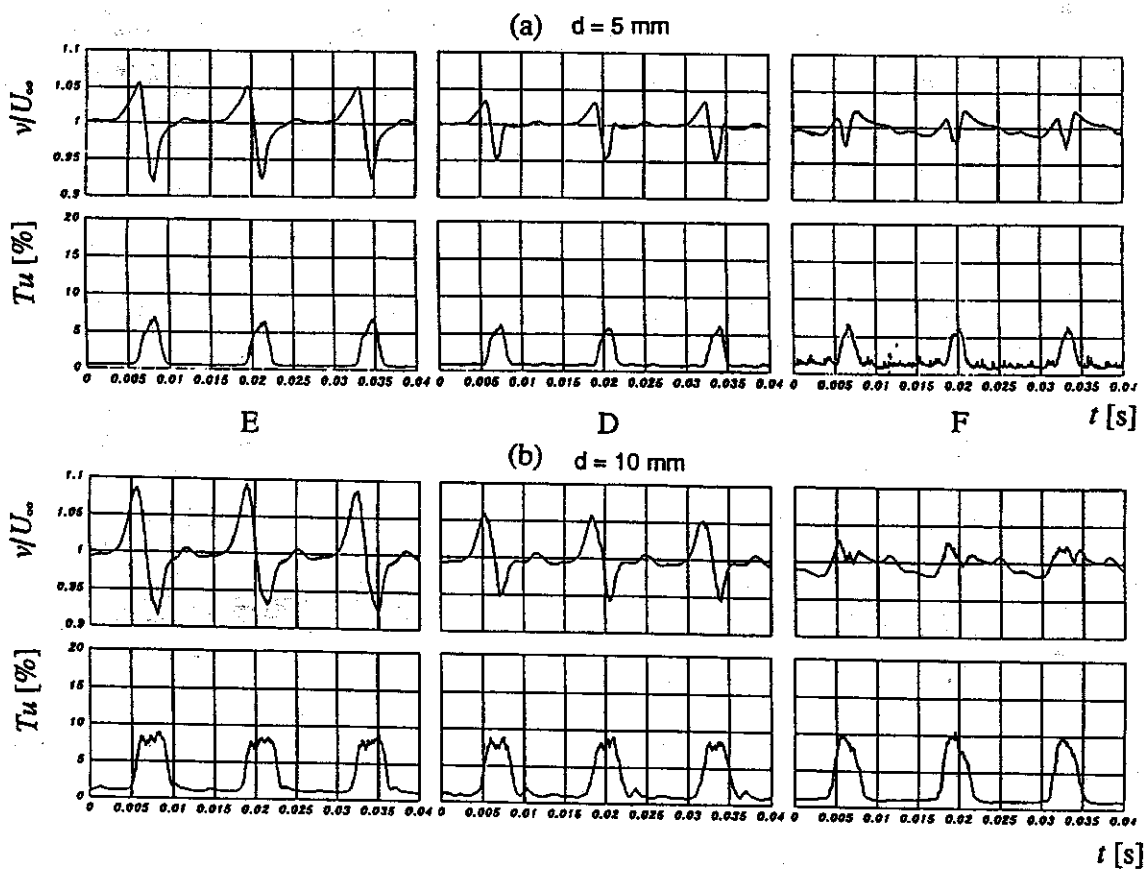

Fig. 7 Effect of the gap between the measuring point and the plate surface on the wake profiles: (*a*) d = 5 mm, (*b*) d = 10 mm

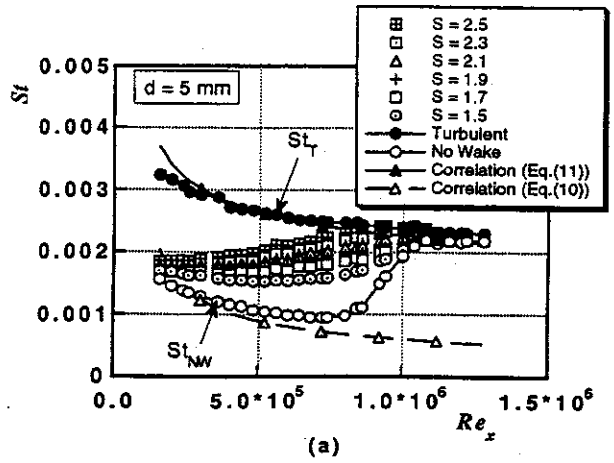

Fig. 8 Stanton number distributions for several Strouhal numbers: (*a*) d = 5 mm, (*b*) d = 10 mm

the plate and the moving cylinders from 0.06 m to 0.24 m. These cases correspond to $X/d \cong 10$ through 40, where X is a distance measured along the relative exit flow direction from the cylinder. Such a wake-affected heat transfer is seemingly most enhanced at $l_D = 0.06$, but the difference among the data in Fig. 12 is not as noticeable as was expected from the enlarged relative distance between the cylinders and the test plate.

Modified Wake-Induced Transition Model

As mentioned above, the published wake-induced transition models need to be modified in order to reproduce the heat

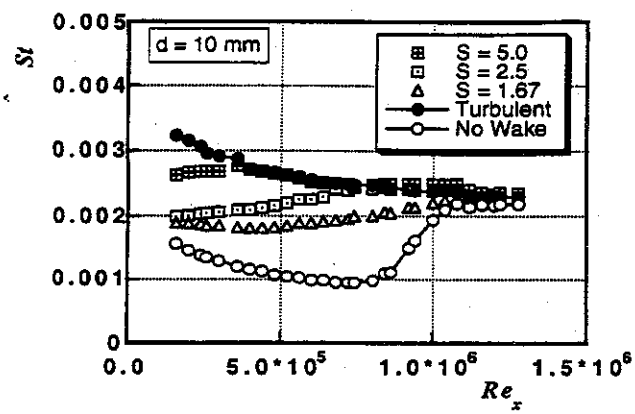

Fig. 9 Stanton number distributions for several Strouhal numbers, including the highest Strouhal number case (d = 10 mm)

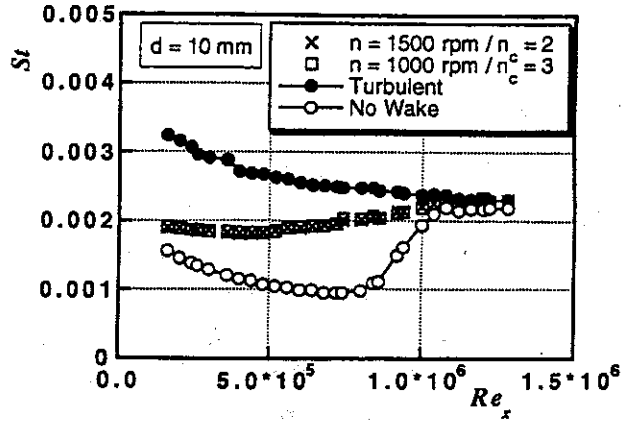

Fig. 10 Dominant effect of the Strouhal number on the heat transfer augmentation by the wake passage

transfer enhancement caused by wakes of larger diameter cylinders. One way to achieve this end is to shift the forced transition point in the upwind direction. Best fitting of the measured intermittency factor, namely

$$\gamma(x) = \frac{\mathrm{St}(x) - \mathrm{St}_{NW}(x)}{\mathrm{St}_T(x) - \mathrm{St}_{NW}(x)}, \qquad (12)$$

with Eq. (2) yields new forced transition points, which are, for the data in Fig. 11, about −0.02 m for 5-mm-dia cylinder and

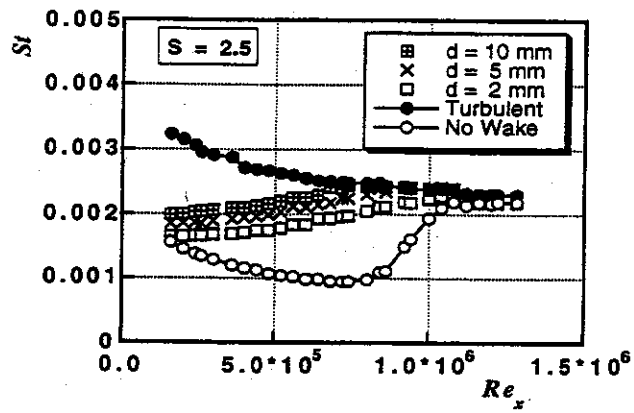

Fig. 11 Effect of the cylinder diameters on the heat transfer (S = 2.5)

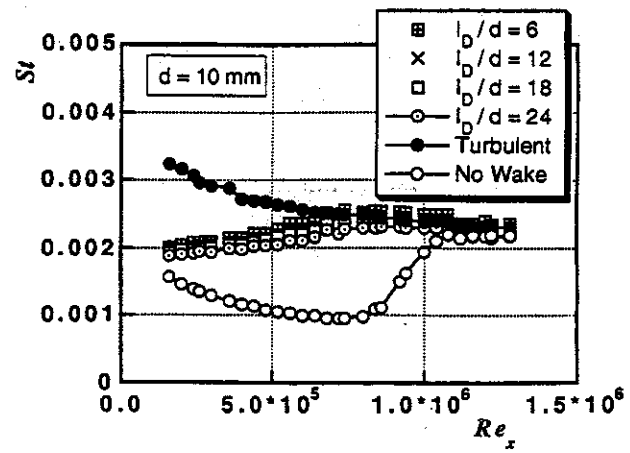

Fig. 12 Effect of the axial distance between the wake-generating cylinders and the plate leading edge upon the heat transfer (S = 2.5)

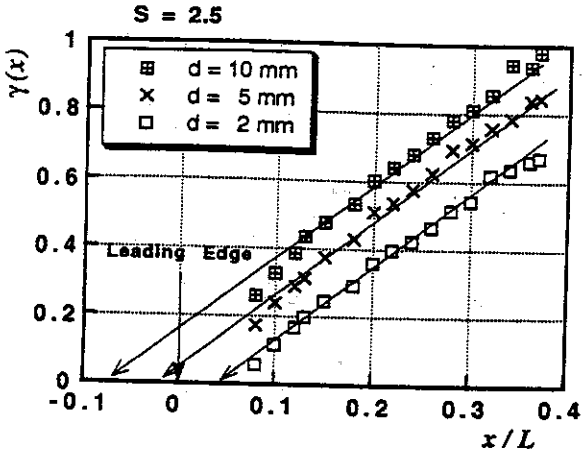

Fig. 13 Intermittency factor plots against the distance from the leading edge

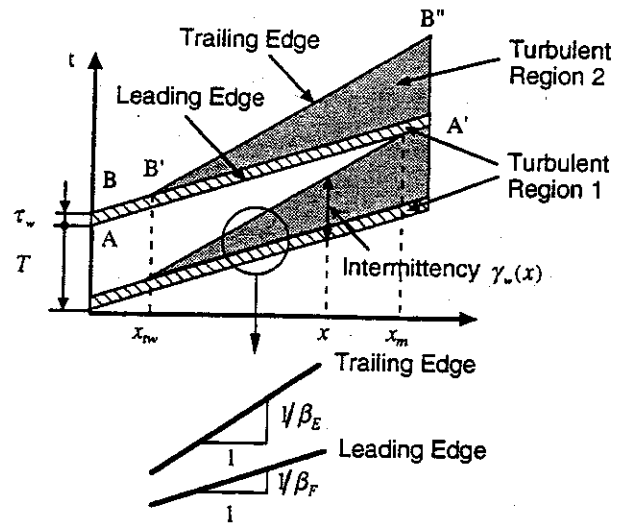

Fig. 14 Schematic of the modified wake-induced transition model in a distance–time diagram

about −0.08 m for 10-mm-dia cylinder as shown in Fig. 13. These negative values indicate that wake-induced transitions start before the plate leading edge, therefore they are unacceptable for wake-induced transition points because they don't have any physical meanings. Thus we must seek another approach for modifying the transition model.

According to Addison and Hodson (1990a, b), the time taken for wake turbulence to diffuse into a laminar boundary layer is very short compared to the wake-passing period. They have shown that the ratio of the diffusion time to the period is approximately represented by the ratio of a molecular kinematic viscosity to a wake-associated eddy viscosity. This means that the boundary layer over which the wake is passing may be immediately activated to become turbulent by the turbulence kinetic energy pouring in. While the laminar boundary layer thickness is very thin and velocity gradient is large, a viscous effect around there is strong enough to dissipate the turbulence kinetic energy quickly, so that the boundary layer is supposed to return to a nondisturbed condition after the wake goes away. This supposition implies that the turbulent state of the boundary layer lasts only for the wake duration, and the wider a wake width, the longer the boundary layer remains turbulent. A similar approach was used by Dullenkopf and Mayle (1994) in order to evaluate the effect of the wake passing on the laminar boundary layer. After the boundary layer grows to some extent, it becomes more susceptible to the turbulence kinetic energy diffused from the wake, then turbulent spots finally emerge inside the boundary layer causing the onset of wake-induced transition.

On the basis of this idea of the wake-induced transition, a distance–time diagram for the boundary layer state under the influence of periodic wakes can be illustrated as shown in Fig. 14. Equation (2) is then modified so as to have the following transition model, namely

$$\gamma_w(x) = \min\,[1, \Gamma(x)]$$

$$\Gamma(x) = \left(\frac{1}{\beta_E} - \frac{1}{\beta_F}\right)\frac{x - x_{tw}}{U_\infty T} + \frac{\tau_w}{T}$$

$$= \left(\frac{1}{\beta_E} - \frac{1}{\beta_F}\right)\frac{x - x_{tw}}{L}\,\mathrm{S} + \frac{\mathrm{S}}{\mathrm{S}_w}, \quad x \geq x_{tw}$$

$$\Gamma(x) = \frac{\mathrm{S}}{\mathrm{S}_w}, \quad x < x_{tw},$$

$$\mathrm{S} = \frac{L}{U_\infty T} \quad \mathrm{S}_w = \frac{L}{U_\infty \tau_w}, \tag{13}$$

where S is the Strouhal number and τ_w is the wake duration. The diagram in Fig. 14, similar to that of Hodson (1990), has several features to be noted. First, the duration of a turbulent region caused just beneath an incoming wake, which we refer to as "Turbulent Region 1," is assumed constant from the plate leading edge throughout to the end of the transition, despite the fact that the wake profile of turbulence intensity suffers from somewhat gradual deformation as observed in the previous section. Second, for simplicity a wake-induced point is defined by the location where another turbulent region referred to as "Turbulent Region 2" appears and starts to follow the preceding wake. This turbulent region 2 has its origin from wake-induced turbulent spots, so that the moving speed of the trailing edge should be the same with that of turbulent spots, i.e., 0.55 U_∞ in this case.

One might feel that the expression for the intermittency by Eq. (13) or the diagram in Fig. 14 is too deterministic when considering the randomness of the transition process as well as of the wake itself. This is critical for determining the onset of the wake-induced transition, as described by Mayle (1991). When averaged, however, the effect of the randomness can be expected to become confined, consequently Eq. (13) works fairly well to predict the wake-affected heat transfer as will be shown later.

The present author is aware that there have been some discussions on the relationship between a wake-induced transition and wake characteristics. One of the latest discussions was made by Cumpsty to the study of Walker (1993), in which they argued about whether the passage of wakes has any direct connection with a forced boundary layer transition. Quoting some experimental findings from the study of Orth (1993), Walker inferred that there existed both direct and indirect mechanisms of the transition caused by the periodic passing wake (or wake turbulence). In the present wake-induced transition model, such indirect mechanisms are not finally taken into account. This is because in the heat transfer measurements of this study, as well as in the second part of the study (Part II), the effect of the indirect mechanism could not be identified. Detailed arguments about the reason for these somewhat conflicting results are made in Part II.

The unknown in Eq. (13), x_{tw} and τ_w, could be determined by a best fitting of the experimental data with the corresponding curves of Eq. (13), but such a straightforward operation seems a very cumbersome task. Whence, an assumption is made about the wake-induced transition point. Addison and Hodson (1990a, b) have found in their experiment using an annular cascade that

Table 1

Cylinder diameter [mm]	Assumed wake duration [msec]
10	3.40
5	1.77
2	0.15

the wake-induced transition starts at the place where a Reynolds number based on momentum thickness, Re_θ, is around 200. This value corresponds to the instability point of the laminar boundary layer with a Blasius-type velocity profile; accordingly, it seems reasonable to use the following relation as a criterion for determining x_{tw}:

$$Re_\theta = 200 \text{ at } x = x_{tw}. \quad (14)$$

In the present case, x_{tw} is about 0.045 m measured from the leading edge. This simple criterion, which implies that a wake-induced transition is determined mainly by the state of time-averaged boundary layer irrespective of wake characteristics, is employed here for convenience. As will be shown in Part II, however, the wake-induced transition point shows a considerable dependency on the wake characteristics, especially by wake duration. Nevertheless, Eq. (14) works fairly well, as shown below.

By means of a best-fit technique with the experimental data, wake duration τ_w is determined for each of the wake-generating cylinders and the results are listed in Table 1. Some comparisons are then made between the experimental heat transfer data and the corresponding estimations by using the proposed transition model of Eq. (13) in conjunction with the relation of

$$St(x) = (1 - \gamma(x))St_{NW}(x) + \gamma(x)St_T(x), \quad (15)$$

where $x_{tw} = 0.045$. Figures 15–18 show the comparisons for three Strouhal number cases. It follows that the experimental data, even at the highest Strouhal number as shown in Fig. 18, are successfully reproduced by the transition model of Eq. (13) and Eq. (15), which indicates the usefulness of the proposed transition model, as well as the assumption for the wake-induced transition point.

In this study, it is shown that the proposed transition model works well to predict the wake-affected heat transfer on the flat plate. Actual flow fields in turbomachines, however, are very complicated compared to that of the present experiment and

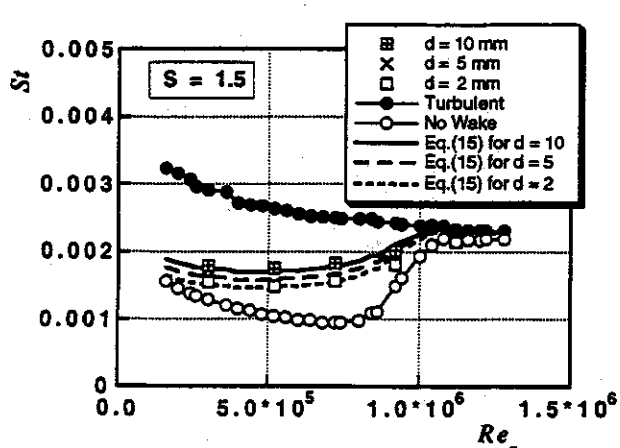

Fig. 15 Comparisons between the estimations by Eq. (15) and the experiments (S = 1.5)

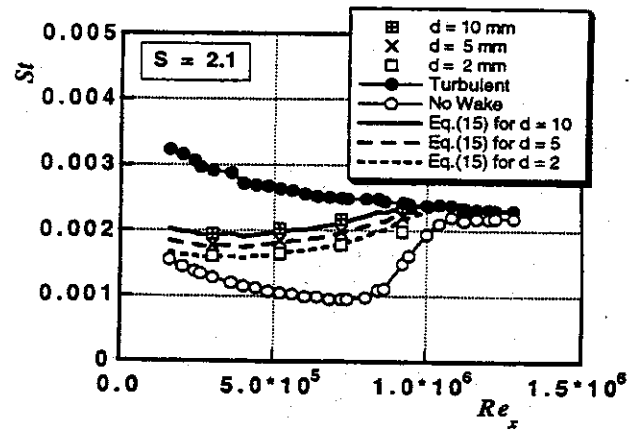

Fig. 16 Comparisons between the estimations by Eq. (15) and the experiments (S = 2.1)

have several factors that are not taken into account in the model, which are for example effects of curvature, pressure gradient, compressibility and so on. Nevertheless, the author believes that the model will do in that case as a basic model of the wake-induced transition, in which the effects of those factors could be incorporated afterward.

Discussion

Examining the experimental data obtained at relatively low Strouhal numbers such as those in Fig. 15, there appear some

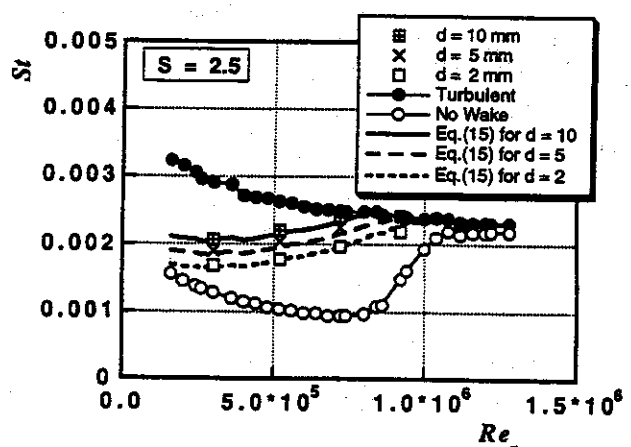

Fig. 17 Comparisons between the estimations by Eq. (15) and the experiments (S = 2.5)

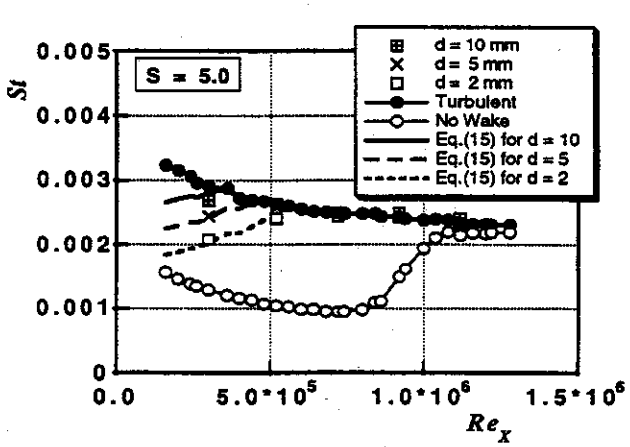

Fig. 18 Comparisons between the estimations by Eq. (15) and the experiments (S = 5.0)

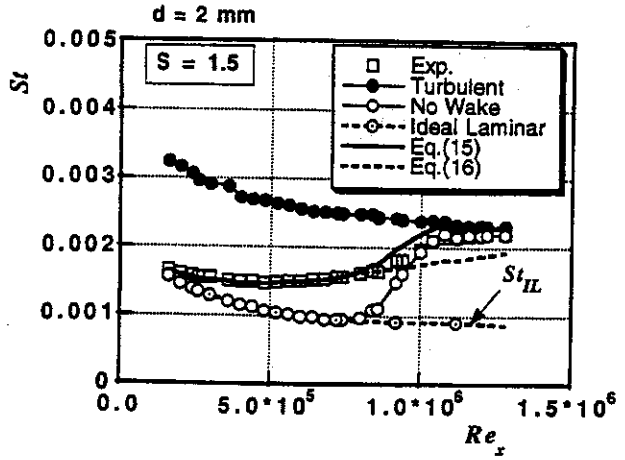

Fig. 19 Estimation of the wake-affected heat transfer by use of data for an ideal laminar boundary layer (S = 1.5)

discrepancies between the data and the estimates near the end of the transition, where the estimated values become larger than the experimental data. At first glance it seemed that such discrepancies were due to the steady heat transfer distributions $St_{NW}(x)$ that contained some effects of the natural transition occurring around there. In order to check this supposition, ideal laminar heat transfer distributions free from the effect of the natural transition, $St_{IL}(x)$ were derived by extending the data smoothly from the natural transition point ($x/L = 0.4$ in this case), and are used in Eq. (15), instead of the measured $St_{NW}(x)$ as follows;

$$St(x) = (1 - \gamma(x))St_{IL}(x) + \gamma(x)St_T(x). \quad (16)$$

Such modified estimations are then compared with the corresponding experimental data for the cylinder of 2 mm, as presented in Figs. 19 and 20. Compared to the experimental data as well as to the corresponding "original" estimations, use of the ideal laminar heat transfer distributions considerably underestimates wake-affected heat transfer when the Strouhal number is low (Fig. 19). As the Strouhal number increases (Fig. 20), newly estimated curves of wake-affected heat transfer gradually tend to follow the experimental data more precisely than the original estimations do. This indicates that the passage of periodic wakes surely influences time-averaged characteristics of the boundary layer as the wake-passing Strouhal number increases and considerably suppresses its natural transition process.

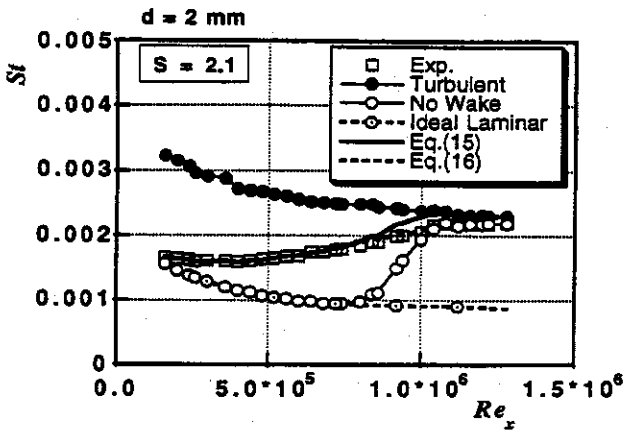

Fig. 20 Estimation of the wake-affected heat transfer by use of data for an ideal laminar boundary layer (S = 2.1, effect of the natural transition on the wake-affected heat transfer is completely suppressed)

Conclusions

Measurements of wake-affected heat transfer distributions on a flat plate are made by use of the wake generator, and a modified wake-induced transition model in terms of intermittency factor is proposed. Findings in this study are summarized as follows;

1 A wake-induced transition model with no consideration of the difference in wake characteristics failed to reproduce the experimental data of wake-affected heat transfer.

2 A modification on the transition model was made in order to incorporate the effects of wake duration. Also proposed was a criterion for a wake-induced transition point, which stated that the transition point corresponded to the place where the momentum thickness Reynolds number was 200.

3 Wake-affected heat transfer distributions for all unsteady flow conditions were well-reproduced by the proposed transition model, where the wake durations were experimentally determined.

4 Small discrepancies between the experiments and the model were recognized over the region where natural transition appeared. It was found that in some cases great improvement on estimation of wake-affected heat transfer was achieved by use of an ideal heat transfer distribution free from natural transition instead of the measured data.

Acknowledgments

This study is supported by IHI, Ishikawajima-Harima Heavy Industries Co., with supervision of S. Yamawaki and R. Henk. Great help in executing all experimental works was provided by K. Meguro and Y. Yamashita and is gratefully acknowledged.

References

Addison, J. S., and Hodson, H. P., 1990a, "Unsteady Transition in an Axial-Flow Turbine: Part I—Measurements on the Turbine Rotor," ASME JOURNAL OF TURBOMACHINERY, Vol. 112, pp. 206–214.

Addison, J. S., and Hodson, H. P., 1990b, "Unsteady Transition in an Axial-Flow Turbine: Part II—Cascade Measurements and Modeling," ASME JOURNAL OF TURBOMACHINERY, Vol. 112, pp. 215–222.

Addison, J. S., and Hodson, H. P., 1992, "Modeling of Unsteady Transition Boundary Layers," ASME JOURNAL OF TURBOMACHINERY, Vol. 114, pp. 580–589.

Dong, Y., and Cumpsty, N. A., 1990, "Compressor Blade Boundary Layers: Part 2—Measurements With Incident Wakes," ASME JOURNAL OF TURBOMACHINERY, Vol. 112, pp. 231–240.

Dullenkopf, K., Schulz, A., and Witting, S., 1991, "The Effect of Incident Wake Conditions on the Mean Heat Transfer of an Airfoil," ASME JOURNAL OF TURBOMACHINERY, Vol. 113, pp. 412–418.

Dullenkopf, K., and Mayle, R. E., 1994, "The Effects of Incident Turbulence and Moving Wakes on Laminar Heat Transfer in Gas Turbine," ASME JOURNAL OF TURBOMACHINERY, Vol. 116, pp. 23–28.

Emmons, H. W., 1951, "The Laminar–Turbulent Transition in a Boundary Layer—Part I," *Journal of Aeronautical Science*, Vol. 18, pp. 490–498.

Funazaki, K., Meguro, T., and Yamawaki, S., 1993, "Studies on the Unsteady Boundary Layer on a Flat Plate Subjected to Incident Wakes (Forced Transition Models of the Boundary Layer)," *JSME International Journal*, Vol. 36, pp. 532–539.

Han, J. C., Zhang, L., and Ou, S., 1993, "Influence of Unsteady Wake on Heat Transfer Coefficient From a Gas Turbine Blade," ASME *Journal of Heat Transfer*, Vol. 115, pp. 904–911.

Hodson, H. P., 1990, "Modeling Unsteady Transition and Its Effect on Profile Loss," ASME JOURNAL OF TURBOMACHINERY, Vol. 112, pp. 619–701.

Kays, W. M., and Crawford, M. E., 1980, *Convective Heat and Mass Transfer*, McGraw-Hill, New York, p. 140.

Kline, S. J., and McClintock, F. A., 1953, "Describing Uncertainties in Single Sample Experiments," *Mechanical Engineering*, Jan., pp. 3–8.

LaGraff, J. E., Ashworth, D. A., and Schultz, D. L., 1989, "Measurement and Modeling of the Gas Turbine Blade Transition Process as Disturbed by Wakes," ASME JOURNAL OF TURBOMACHINERY, Vol. 111, pp. 315–322.

Mayle, R. E., 1991, "The Role of Laminar-Turbulent Transition in Gas Turbine Engines," ASME JOURNAL OF TURBOMACHINERY, Vol. 113, pp. 509–537.

Mayle, R. E., and Dullenkopf, K., 1990, "A Theory for Wake-Induced Transition," ASME JOURNAL OF TURBOMACHINERY, Vol. 112, pp. 188–195.

Mayle, R. E., and Dullenkopf, K., 1991, "More on the Turbulent-Strip Theory for Wake-Induced Transition," ASME JOURNAL OF TURBOMACHINERY, Vol. 113, pp. 428–432.

Meyer, R. X., 1957, "The Effect of Wakes on the Transient Pressure and Velocity Distributions in Turbomachines," ASME *Journal of Basic Engineering*, Vol. 80, pp. 1544–1552.

Orth, U., 1993, "Unsteady Boundary-Layer Transition in Flow Periodically Disturbed by Wakes," ASME JOURNAL OF TURBOMACHINERY, Vol. 115, pp. 707–713.

Pfeil, H., and Herbst, R., 1979, "Transition Procedure of Instationary Boundary Layer," ASME Paper No. 79-GT-128.

Pfeil, H., Herbst, R., and Schroder, T., 1983, "Investigation of the Laminar–Turbulent Transition of Boundary Layers Disturbed by Wakes," ASME *Journal of Engineering for Power*, Vol. 105, pp. 130–137.

Walker, G. J., 1993, "The Role of Laminar–Turbulent Transition in Gas Turbine Engines: A Discussion," ASME JOURNAL OF TURBOMACHINERY, Vol. 115, pp. 207–217.